Cell Death and Differentiation (2012) 19, 562–572
© 2012 Macmillan Publishers Limited All rights reserved 1350-9047/12
www.nature.com/cdd

Silencing or knocking out the Na^+/Ca^{2+} exchanger-3 (NCX3) impairs oligodendrocyte differentiation

F Boscia[1], C D'Avanzo[2], A Pannaccione[2], A Secondo[2], A Casamassa[2], L Formisano[2], N Guida[2] and L Annunziato*[,1,2]

Changes in intracellular $[Ca^{2+}]_i$ levels have been shown to influence developmental processes that accompany the transition of human oligodendrocyte precursor cells (OPCs) into mature myelinating oligodendrocytes and are required for the initiation of the myelination and re-myelination processes. In the present study, we explored whether calcium signals mediated by the selective sodium calcium exchanger (NCX) family members NCX1, NCX2, and NCX3, play a role in oligodendrocyte maturation. Functional studies, as well as mRNA and protein expression analyses, revealed that NCX1 and NCX3, but not NCX2, were divergently modulated during OPC differentiation into oligodendrocyte phenotype. In fact, whereas NCX1 was downregulated, NCX3 was strongly upregulated during oligodendrocyte development. The importance of calcium signaling mediated by NCX3 during oligodendrocyte maturation was supported by several findings. Indeed, whereas knocking down the NCX3 isoform in OPCs prevented the upregulation of the myelin protein markers 2′,3′-cyclic nucleotide-3′-phosphodiesterase (CNPase) and myelin basic protein (MBP), its overexpression induced an upregulation of CNPase and MBP. Furthermore, NCX3-knockout mice showed not only a reduced size of spinal cord but also marked hypo-myelination, as revealed by decrease in MBP expression and by an accompanying increase in OPC number. Collectively, our findings indicate that calcium signaling mediated by NCX3 has a crucial role in oligodendrocyte maturation and myelin formation.
Cell Death and Differentiation (2012) **19,** 562–572; doi:10.1038/cdd.2011.125; published online 30 September 2011

Oligodendrocytes, the myelin-forming cells of the CNS, arise from oligodendrocyte precursor cells (OPCs) that colonize both the gray and the white brain matter during development.[1] Although many OPCs differentiate into mature myelinating oligodendrocytes during the early and much later stages of human brain development, a considerable number of them do persist in the adult brain, and may provide a source of new oligodendrocytes, as well as protoplasmic astrocytes and neurons.[2,3] Because of their apparent stem-like characteristics, adult OPCs have recently gained much attention, for they are regarded as a potential reservoir of cells capable of self-renewal, differentiation, and re-myelination after CNS injury.[4] Thus, understanding how oligodendrocyte development proceeds and what factors govern the differentiation fate of OPCs is crucial to discover new effective therapeutic targets for de-myelinating diseases such as multiple sclerosis (MS).

Changes in intracellular calcium levels have a critical role in OPC migration, lineage progression, and differentiation; furthermore, they are required for myelination and re-myelination processes.[5–7] The Na^+/Ca^{2+} exchanger (NCX),[8] a transmembrane domain protein, which, by operating in a bidirectional way, couples the efflux of Ca^{2+} to the influx of Na^+ into the cell or, vice versa, the influx of Ca^{2+} to the efflux of Na^+, is involved in the regulation of diverse neuronal and glial cell functions.[8,9] Furthermore, NCX is involved in regulating intracellular Ca^{2+} concentration under pathological conditions and has been proposed as a potential therapeutic target in different disorders of the nervous system, including de-myelinating conditions such as MS,[10,11] ischemia–reperfusion injury,[12–14] and spinal cord injury.[15,16] Three different ncx1, ncx2, and ncx3 genes have been identified in mammals.[17–19] Although the expression of the different NCX mRNAs in oligodendrocytes has been described,[20] their role during oligodendrocyte development has never been investigated.

In the present study, we asked whether the three NCX isoforms, by modulating Na^+ and Ca^{2+} homeostasis, might be involved in OPC maturation and myelin formation. To address these questions, we first examined their expression and, then, by using a patch clamp in whole-cell configuration and single-cell FURA-2 microfluorimetry, we studied their functional activity during oligodendrocyte and astrocyte development either in the human oligodendrocyte progenitor MO3.13 cell line or in primary rat OPC cultures. We found that NCX3 was strongly upregulated during oligodendrocyte development, whereas NCX1 was downregulated. Next, the effect of NCX3 silencing on myelin formation was evaluated by using an short-interfering RNA (siRNA) strategy or transgenic NCX3-knockout mice. Finally, the effect of NCX3

[1]Fondazione IRCSS SDN, Naples, Italy and [2]Division of Pharmacology, Department of Neuroscience, School of Medicine, 'Federico II' University of Naples, Naples, Italy
*Corresponding author: L Annunziato, Department of Neuroscience, Division of Pharmacology, School of Medicine, 'Federico II' University of Naples, Via Pansini 5, Naples 80131, Italy. Tel: +39 81 746 3318; Fax: +39 81 746 3323; E-mail: lannunzi@unina.it
Keywords: oligodendrocyte precursor cells (OPCs); oligodendrocyte; Na^+/Ca^{2+} exchanger; NCX3; myelin
Abbreviations: bFGF, basic fibroblast growth factor; BrdU, 5-bromo-2′-deoxyuridine; CNPase, 2′,3′-cyclic nucleotide-3′-phosphodiesterase; DIVs, days *in vitro*; DMEM, Dulbecco's modified Eagle's medium; FBS, fetal bovine serum; GFAP, glial fibrillary acidic protein; MAG, myelin-associated glycoprotein; MBP, myelin basic protein; MS, multiple sclerosis; NCX, Na^+/Ca^{2+} exchanger; NF200, neurofilament 200 kDa; NG2, chondroitin sulfate proteoglycan; OPCs, oligodendrocyte precursor cells; PDGF, platelet-derived growth factor; PMA, 4-b-phorbol-12-myristate-13-acetate; RT, room temperature; T3, triiodothyronine; T4, thyroxine
Received 12.5.11; revised 27.7.11; accepted 20.8.11; Edited by P Bouillet; published online 30.9.11

overexpression on myelin formation was examined by transfecting oligodendrocyte MO3.13 precursors with a plasmid construct expressing NCX3–Flag. Our findings indicate that the NCX3 isoform has a relevant role during oligodendrocyte development.

Results

Changes in $[Ca^{2+}]_i$ levels are involved in the transformation of MO3.13 progenitor cells into oligodendrocytes but not into astrocytes. When human oligodendrocyte MO3.13 progenitor cells were cultured in serum-free medium in the presence of 100 nM 4-b-phorbol-12-myristate-13-acetate (PMA) for 7 days, an upregulation of oligodendrocyte lineage markers was observed (Figure 1). In particular, confocally detected myelin basic protein (MBP) immunoreactivity, an index of myelin expression, intensely augmented in the cytosol of differentiated cells at 7 days when compared with control undifferentiated cells (Figure 1A, a and f). In these undifferentiated cells, MBP expression was mainly confined to the Golgi compartment, as demonstrated by the colocalization of MBP with the Golgi marker, Golgin-97 (Figure 1A, b–e). By contrast, no myelin expression was found in the Golgi compartment of differentiated cells, as no colocalization of MBP with Golgin-97 was observed (data not shown). Similarly, western blot experiments revealed that the protein levels of the other two oligodendrocyte markers, 2′,3′-cyclic nucleotide-3′-phosphodiesterase (CNPase) and myelin-associated glycoprotein (MAG), increased significantly within 7 days (Figures 1B and C). Conversely, exposure of MO3.13 progenitor cells to 100 nM PMA progressively downregulated the protein expression of both the astrocyte markers, S100B and glial fibrillary acidic protein (GFAP), as well as the OPC marker, namely the chondroitin sulfate proteoglycan, NG2 (Figure 1D). Interestingly, $[Ca^{2+}]_i$, evaluated by single-cell microfluorimetric analysis, was significantly upregulated in a time-dependent manner during oligodendrocyte progression (Figure 1E).

When human oligodendrocyte MO3.13 progenitor cells were cultured for 7 days in the presence of 10% fetal bovine serum (FBS) but in the absence of PMA, an upregulation of the astrocyte marker S100B was observed (Figures 2A and B). Colocalization experiments with anti-S100B and anti-MBP antibodies indicated an intense co-expression of the two proteins in the perinuclear compartment of undifferentiated progenitors (Figure 2A, a–d). S100B

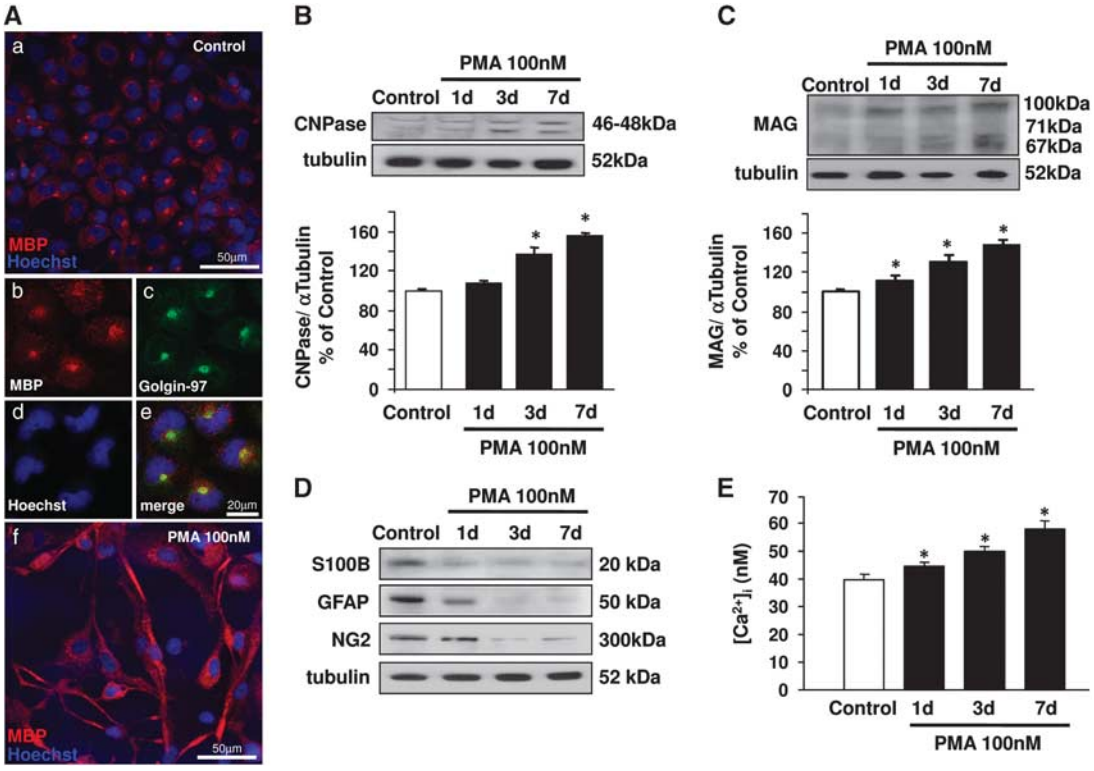

Figure 1 Oligodendrocyte and astrocyte markers, and intracellular $[Ca^{2+}]_i$ levels, in oligodendrocyte MO3.13 progenitor cells differentiated into an oligodendrocyte phenotype. (**A**) Confocal immunofluorescence images showing MBP immunosignal in MO3.13 cells under control conditions (a) and after differentiation (f) with 100 nM PMA for 7 days. Colocalization analysis of MBP with Golgin-97 in undifferentiated cells is shown in panels b–e. Scale bars: a and f: 50 μm; b–e: 20 μm (**B** and **C**), Western blot and densitometric analysis of CNPase (**B**) and MAG (**C**) protein levels in MO3.13 cells under control conditions and after differentiation with 100 nM PMA for 1, 3, and 7 days. Quantifications were performed on the sum of the two CNP-specific enhanced chemiluminescence bands of 46 and 48 kDa, or of the three MAG-specific bands of 100, 71, and 67 kDa. Data were normalized on the basis of α-tubulin levels and expressed as percentage of controls. The values represent the means ± S.E.M. ($n = 3$–4). *$P < 0.05$ *versus* controls. (**D**) Western blot analysis of S100B (upper), GFAP (middle), and NG2 (lower) protein levels in MO3.13 cells under control conditions and after differentiation with 100 nM PMA for 1, 3, and 7 days. (**E**) Quantification of $[Ca^{2+}]_i$ detected with FURA-2AM in MO3.13 cells under control conditions and after differentiation with 100 nM PMA for 1, 3, and 7 days. Each bar represents the mean ± S.E.M. of the data obtained from 60 cells per group in three independent experimental sessions. *$P < 0.05$ *versus* control

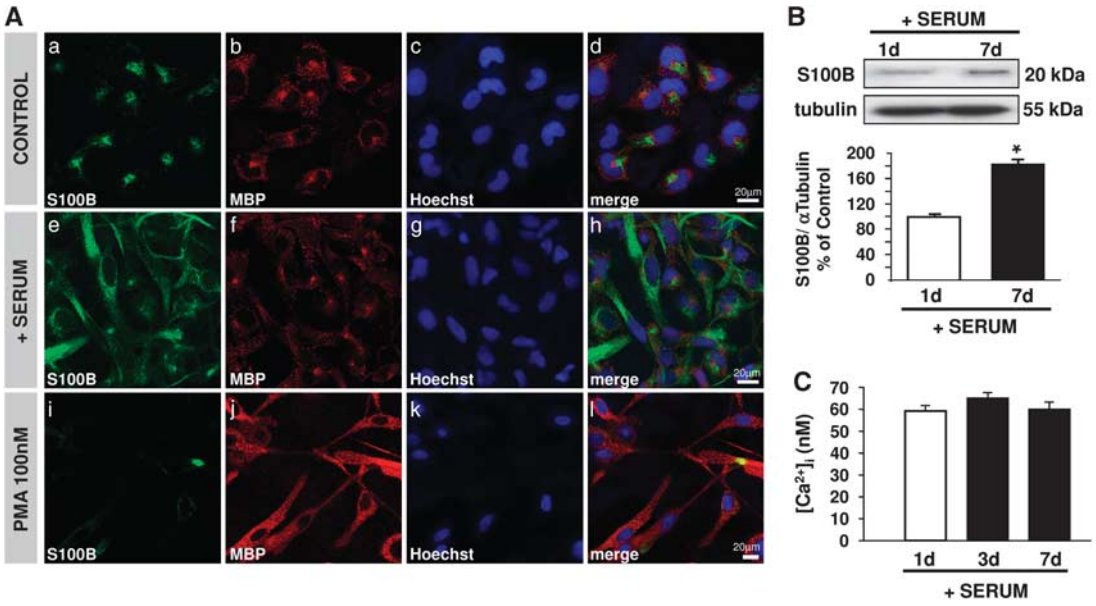

Figure 2 Oligodendrocyte and astrocyte markers, and intracellular $[Ca^{2+}]_i$ levels, in oligodendrocyte MO3.13 progenitor cells differentiated into astrocyte phenotype. (**A**) Confocal double immunofluorescence images showing both S100B and MBP immunosignals in MO3.13 cells under control conditions (a–d) and after differentiation with serum for 7 days (e–h) or with 100 nM PMA for 7 days (i–l). Scale bars: a–l: 20 μm. The magnification of panels (a–h) is higher than that of panels (i–l). Although the scale bar in all the panels is 20 μm, in the last three panels (i–l) the length of the bar is approximately one-half. (**B**) Western blot and densitometric analysis of S100B protein levels in MO3.13 cells under control conditions and after differentiation with serum for 7 days. The values represent the means ± S.E.M. ($n = 3$–4). *$P < 0.05$ *versus* control. (**C**) Quantification of $[Ca^{2+}]_i$ detected with FURA-2AM in MO3.13 cells under control conditions and after differentiation with serum for 1, 3, and 7 days. Each bar represents the mean ± S.E.M. of the data obtained from 60 cells per group in three independent experimental sessions

immunoreactivity, but not that of MBP, increased after 7 days of serum exposure (Figure 2A, e–h). By contrast, 7 days after PMA incubation, the S100B immunosignal was barely detectable, whereas MBP immunoreactivity was largely upregulated (Figure 2A, i–l). Interestingly, no significant alterations in $[Ca^{2+}]_i$ levels were detected during the differentiation of progenitor cells into astrocytes (Figure 2C).

NCX functional activity is upregulated during differentiation of MO3.13 progenitors into oligodendrocytes. To assess whether NCX might contribute to the changes in $[Ca^{2+}]_i$ levels observed during development of OPCs,[21] changes in NCX activity occurring in MO3.13 cells upon differentiation were recorded by a patch clamp in whole-cell configuration and FURA-2 microfluorimetry. I_{NCX} currents, recorded both in the reverse and forward modes of operation, were significantly higher in oligodendrocytes after 3 and 7 days of differentiation than in controls and at 1 day of PMA exposure. At this time point, the current carried by NCX was significantly lower than that recorded in undifferentiated cells (Figure 3A). Consistently, single-cell FURA-2 video-imaging revealed an upregulation of NCX function when MO3.13 cells differentiated into an oligodendrocyte phenotype after 3 and 7 days of PMA exposure (Figure 3B). Conversely, a significant reduction of NCX activity, measured as Na^+-free-induced Ca^{2+} increase (i.e., reverse mode), occurred in MO3.13 cells exposed for 7 days to serum and therefore differentiated into astrocytes (Figure 3C).

NCX1 and NCX3 transcripts and proteins are differently modulated during differentiation of OPCs into oligodendrocytes. We examined the contribution of each NCX isoform to the changes in NCX activity detected by electrophysiology and microfluorimetry during the differentiation of MO3.13 precursor cells into oligodendrocytes. Quantitative RT-PCR and western blot experiments revealed that a divergent and time-dependent modulation of NCX1 and NCX3 transcripts and protein levels occurred during oligodendrocyte maturation. Indeed, when MO3.13 cells were exposed to 100 nM PMA, a significant increase in NCX3 transcripts and protein levels was observed at 3 and 7 days, at variance with NCX1, whose mRNA and protein expression significantly and progressively decreased within 7 days after exposure (Figures 4A and B). In accordance with mRNA and biochemical studies, confocal immuno fluorescence staining revealed that 7 days of PMA exposure induced a pronounced labeling of the NCX3 isoform (Figure 4C). In fact, NCX3 immunoreactivity, which was confined to the perinuclear compartment of undifferentiated cells (Figure 4C, c and e), was intensely detected along the plasma membrane and in the cytosol of differentiated cells (Figure 4C, d–g). Conversely, NCX1 immunosignal, mainly expressed along the plasma membrane of undifferentiated cells (Figure 4C, a), was undetectable after 7 days of PMA-induced differentiation (Figure 4C, b). No changes in NCX2 transcripts and protein levels were observed during oligodendrocyte development (Figures 4A and C, a and b).

Changes in NCX1 and NCX3 expression and functional activity observed in human oligodendrocyte MO3.13 cells were verified in rat primary cultures of OPCs. For this purpose, OPCs were maintained in a proliferative state in the presence of the two mitogens, platelet-derived growth factor (PDGF)-AA

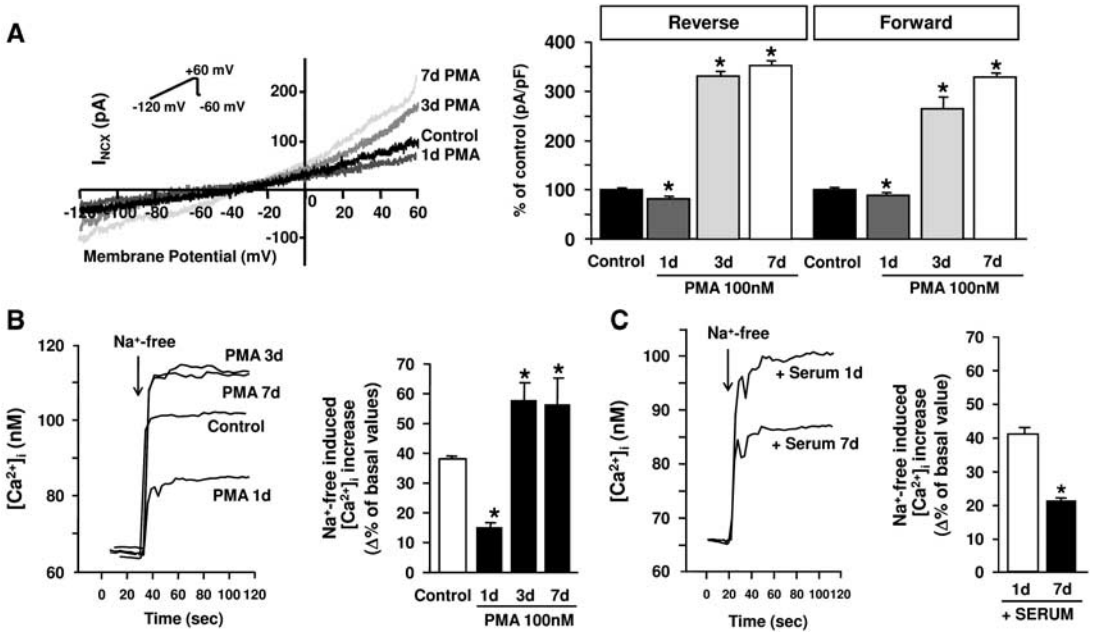

Figure 3 NCX activity in MO3.13 progenitor cells differentiated into oligodendrocyte or astrocyte phenotypes. (**A**, left panel) I_{NCX}-superimposed traces recorded from MO3.13 cells under control conditions (black trace) and after PMA exposure for 1, 3, and 7 days (gray traces). (**A**, right panel) I_{NCX} quantification is expressed as current densities recorded in control and differentiated MO3.13 cells. Each bar represents the mean ± S.E.M. of the data obtained from 20 cells per group in three independent experimental sessions. *$P<0.05$ *versus* control. (**B**, left panel) Superimposed single-cell traces representative of the effect of Na^+-free on $[Ca^{2+}]_i$ detected with FURA-2AM in MO3.13 cells under control conditions and after 100 nM PMA exposure for 1, 3, and 7 days. (**B**, right panel) Quantification of Na^+-free induced $[Ca^{2+}]_i$ increase measured as Δ% of peak *versus* basal values in MO3.13 cells under control conditions and after 100 nM PMA exposure for 1, 3, and 7 days. Each bar represents the mean ± S.E.M. of the data obtained from 60 cells per group in three independent experimental sessions. *$P<0.05$ *versus* control. (**C**, left panel) Superimposed single-cell traces representative of the effect of Na^+-free on $[Ca^{2+}]_i$ detected with FURA-2AM in MO3.13 cells under control conditions and after serum exposure for 7 days. (**C**, right panel) Quantification of Na^+-free induced $[Ca^{2+}]_i$ increase measured as Δ% of peak *versus* basal values in MO3.13 cells under control conditions and after serum exposure for 7 days. Each bar represents the mean ± S.E.M. of the data obtained from 60 cells per group in three independent experimental sessions. *$P<0.05$ *versus* 1d

plus basic fibroblast growth factor (bFGF), and then differentiated into an oligodendrocyte phenotype in the presence of the thyroid hormones triiodothyronine (T3) and thyroxine (T4) for 7 days (Supplementary Figures S1, A and B). Patch-clamp experiments performed at 1, 3, and 7 days during oligodendrocyte differentiation of rat primary OPCs revealed that the currents carried by NCX both in the forward and reverse modes of operation were significantly up-regulated when compared to undifferentiated cells (Figure 5A). Confocal immunofluorescence experiments revealed that NCX1 was highly expressed in primary NG2-positive OPCs (Figure 5B, a–d), but robustly down-regulated in thyroid hormone-differentiated, CNPase-positive oligodendrocytes (Figure 5B, i–l). By contrast, the NCX3 immunosignal, which was scarcely detected in NG2-positive progenitors (Figure 5B, e–h), appeared intensely expressed in differentiated, MAG-positive oligodendrocytes (Figure 5B, m–p).

NCX3 silencing or NCX3 overexpression alters myelin markers in human MO3.13 oligodendrocytes. To establish whether the NCX3 isoform had a role in oligodendrocyte and myelin formation, we knocked down NCX3 using two selective siRNAs (siNCX3 #7 and siNCX3 #8) in MO3.13 progenitor cells. Both siRNAs significantly reduced NCX3 protein and I_{NCX} activity, as revealed by western blot analysis and FURA-2 microfluorimetry (Figures 6A and B). The siNCX3-transfected cells showed a lower expression of the myelin marker CNPase when compared with control or non-targeting siRNA (siControl)-transfected cells differentiated with PMA for 4 days (Figure 6C). The upregulation of MBP immunoreactivity, revealed by immunofluorescence analysis, was also prevented in cells differentiated with PMA and previously transfected with siNCX3 (Figure 6D).

To investigate whether expression of NCX3 was sufficient to induce the expression of myelin proteins, we transfected MO3.13 cells with either a plasmid encoding NCX3–Flag or an empty control vector. The efficiency of NCX3 transfection was evaluated by analyzing the protein levels using anti-Flag or anti-NCX3 antibodies, and by analyzing (Figure 7A) functional activity (Figure 7B). Cells transfected with NCX3–Flag and cultured without PMA had significantly upregulated CNPase protein levels, an effect that was significant 4 days after transfection (Figure 7C). In accordance, colocalization experiments using anti-Flag and anti-MBP antibodies revealed an intense and diffuse MBP immunosignal only within elongated NCX3–Flag-transfected cells (Figure 7D), whereas the MBP immunosignal remained confined to the perinuclear level in the non-transfected cells (arrowheads).

Next, to investigate whether ncx3 overexpression might be associated with an altered state of proliferation, we performed quantitative 5-bromo-2′-deoxyuridine (BrdU) immunohistochemistry to visualize proliferating cells in control, PMA-exposed, or NCX3–Flag-transfected cells. Interestingly, a significant reduction in the number of proliferating cells

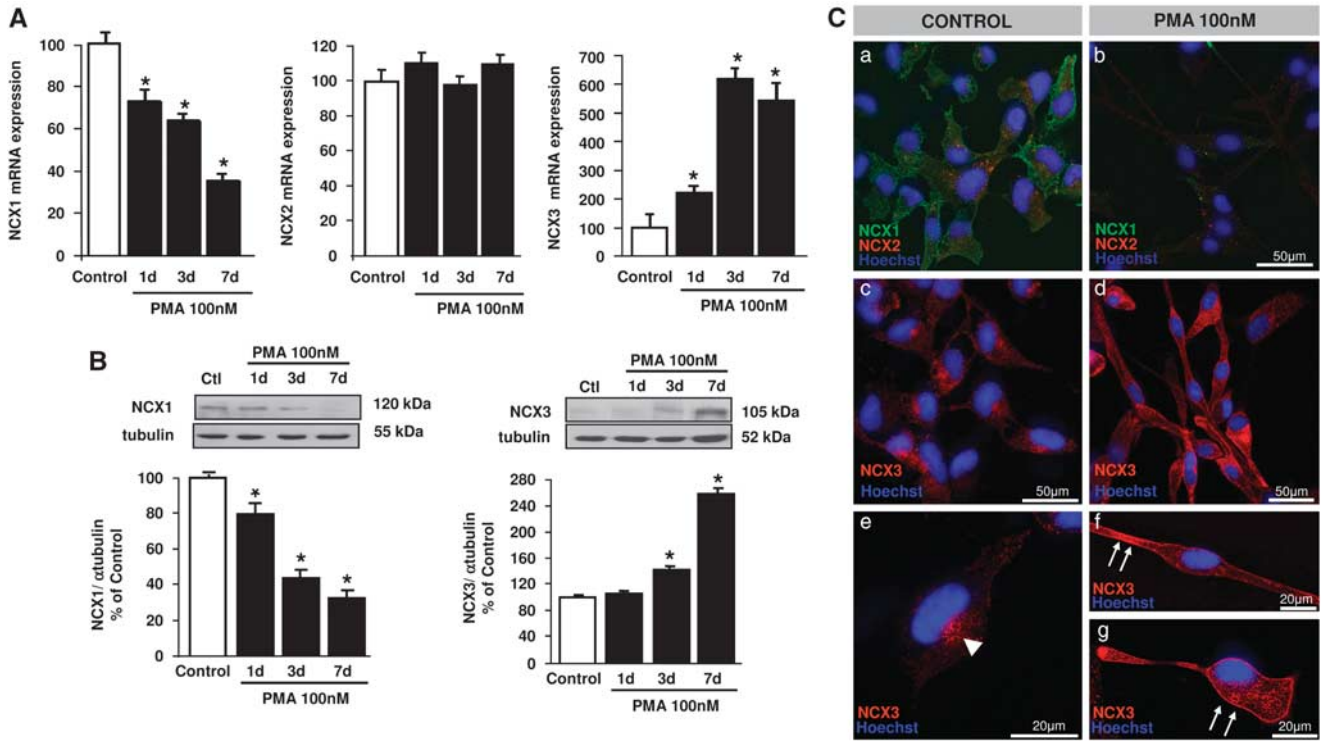

Figure 4 NCX1, NCX2, and NCX3 expression in MO3.13 progenitor cells differentiated into an oligodendrocyte phenotype. (**A**) Real-time PCR of NCX1 (left), NCX2 (middle), and NCX3 (right) mRNA expression in MO3.13 cells under control conditions and after 100 nM PMA exposure for 1, 3, and 7 days. The data were normalized on the basis of the ribosomal L-19 levels and expressed as percentage of controls. The values represent the means ± S.E.M. ($n=4$). *$P<0.05$ *versus* controls. (**B**) Western blot and densitometric analysis of NCX1 (left) and NCX3 (right) protein levels in MO3.13 cells under control conditions and after 100 nM PMA exposure for 1, 3, and 7 days. The data were normalized on the basis of α-tubulin levels and expressed as percentage of controls. The values represent the means ± S.E.M. ($n=3$–4). *$P<0.05$ *versus* controls. (**C**, a–b) Confocal microscopic images showing both NCX1 (green) and NCX2 (red) immunoreactivity in control (a) and differentiated (b) MO3.13 cells. (**C**, c–g) Confocal microscopic images showing NCX3 immunosignal in control (c, e) and PMA-differentiated (d, f, g) MO3.13 cells. The arrowheads in panel e indicate the perinuclear NCX3 immunoreactivity in control cells. The arrows in panels f and g indicate the intense NCX3 labeling along the plasma membrane of PMA-differentiated cells. Scale bars: a–d: 50 μm; e–g: 20 μm

was observed in cells exposed to PMA or transfected with NCX3–Flag when compared with controls (Figure 7E).

ncx3$^{-/-}$ mice show a reduction in myelin expression and axons, and an increased number of OPCs, in the spinal cord. To assess whether NCX3 might have a role in CNS myelination, we analyzed the expression of myelin markers in the oligodendrocytes of mice lacking NCX3, an animal model that has been extensively characterized in our laboratory as well as in others.[22,14,23] For instance, our previous western blot analyses in brain tissue homogenates from ncx3$^{+/+}$ and ncx3$^{-/-}$ mice have revealed no detectable NCX3 protein levels in ncx3-null mice.[14,23] Colocalization experiments, performed using the neuronal marker NeuN or the oligodendrocyte marker MBP in the presence of the NCX3 antibody, revealed that the NCX3 protein was expressed both in the gray and the white matter of the spinal cord of congenic, wild-type, ncx3$^{+/+}$ mice (Figure 8A). Interestingly, spinal cords isolated from ncx3$^{-/-}$ mice were smaller than those isolated from wild-type, congenic, ncx3$^{+/+}$ mice (Figure 8B). Immunoblot analysis for the myelin markers CNPase and MBP in homogenates from spinal cord revealed that both oligodendrocyte markers were reduced in ncx3$^{-/-}$ mice when compared with congenic ncx3$^{+/+}$ mice (Figure 8C, left). By contrast, western blot analysis revealed that the oligodendrocyte progenitor cell marker NG2, but not the astrocyte marker GFAP, was upregulated in ncx3$^{-/-}$ mice. Relevantly, immunoblotting for neurofilament 200 kDa (NF200) revealed that the expression of this axonal neurofilament marker was decreased in ncx3$^{-/-}$ mice when compared with ncx3$^{+/+}$ mice (Figure 8C, right). Quantitative immunofluorescence analysis performed in the white matter of the spinal cord showed a significant reduction in MBP and NF200 fluorescence intensity in ncx3$^{-/-}$ mice when compared with ncx3$^{+/+}$ mice (Figure 8D, a–f). Furthermore, confocal analysis revealed that the number of precursor cells, positive for NG2, was significantly higher in the white matter of the spinal cord of ncx3$^{-/-}$ mice than in ncx3$^{+/+}$ mice (Figure 8D, g–i).

Discussion

The present study demonstrates that the NCX3 isoform of the Na^+/Ca^{2+} exchanger has a crucial role in the progression of OPCs into mature oligodendrocytes, and that NCX3-deficient mice show a reduction of myelinating oligodendrocyte markers in the white matter of the spinal cord. Analysis

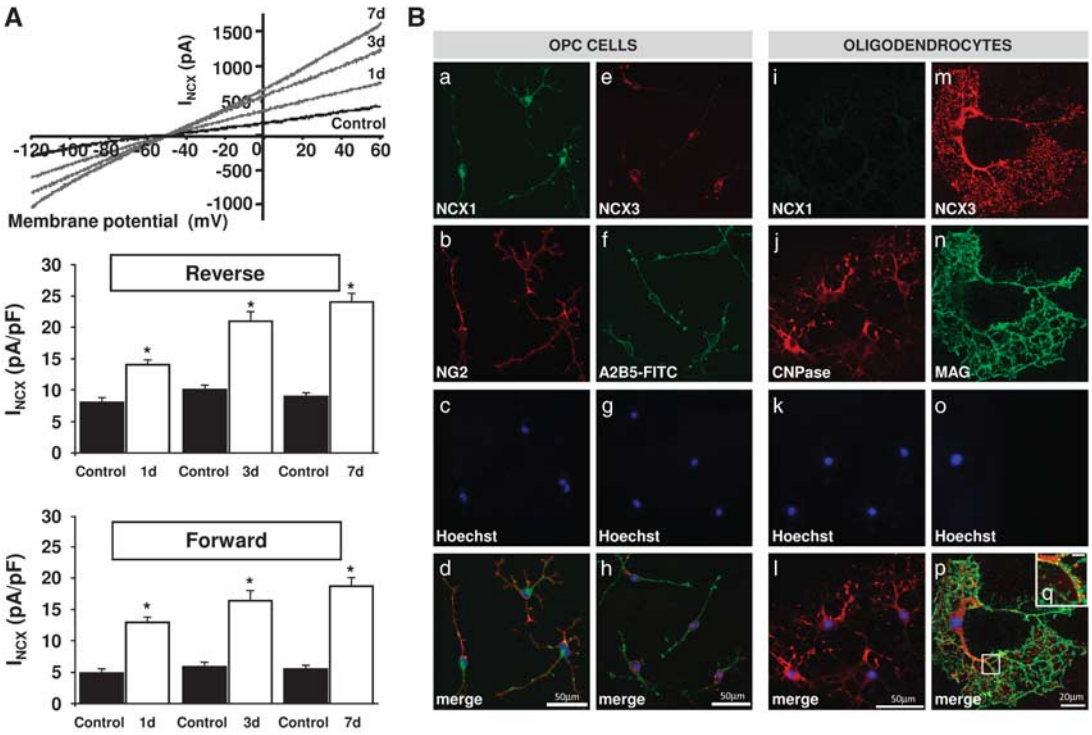

Figure 5 NCX activity in rat primary OPCs differentiated into oligodendrocyte phenotypes. (**A**, upper panel) I_{NCX}-superimposed traces recorded from undifferentiated rat primary OPCs (black trace) and oligodendrocytes differentiated for 1, 3, and 7 days (gray traces). (**A**, middle and lower panels) I_{NCX} quantification is expressed as current densities recorded in control and differentiated OPCs. Each bar represents the mean ± S.E.M. of the data obtained from 20 cells per group in three independent experimental sessions. $^*P<0.05$ *versus* control. (**B**) Colocalization of NCX1 (green) with NG2 (red) in OPCs (a–d) or with CNPase (red) in differentiated oligodendrocytes (i–l). Colocalization of NCX3 (red) with A2B5–FITC (green) in undifferentiated OPCs (e–h) or with MAG (green) in differentiated oligodendrocytes (m–q). A higher magnification of the frame depicted in panel p is shown in panel q. Scale bars: a–l: 50 μm; m–p: 20 μm; q: 5 μm

of mRNA and protein expression in the MO3.13 cell line or primary cultures established that both NCX1 and NCX3 isoforms are differently expressed in OPCs and are divergently modulated during differentiation of OPCs into oligodendrocytes. Indeed, whereas the NCX1 isoform decreased, the NCX3 isoform was strongly increased during oligodendrocyte maturation. The correlation of the expression and functional activity of NCX suggests that NCX1, the only isoform expressed on the plasma membrane of OPCs, represents the main contributor to I_{NCX} recorded in these precursor elements. In accordance with our results, Tong *et al.*[24] have shown that NCX1, but not NCX2, is highly expressed in OPCs and that pharmacological inhibition of NCX1 or its selective silencing with siRNA largely inhibits migration and GABA-induced Ca^{2+} signaling in cultured OPCs.

The most interesting finding of our study indicated that NCX3 represents the only isoform of the exchanger that is upregulated during oligodendrocyte differentiation and the main isoform that is expressed in mature oligodendrocyte. In addition, our evidence showing that, during oligodendrocyte differentiation, NCX3 silencing was able to prevent NCX activity by about 80%, suggests that this exchanger isoform represents the main contributor to NCX activity recorded in these cells. Although the cellular mechanisms underlying the temporal changes of NCX expression and activity still remain to be clarified, it has been documented that either PDGF exposure or protein kinase-C activation, protein factors markedly involved in OPC proliferation and oligodendrocyte formation,[1] stimulate NCX activity in smooth muscle cells and cardiomyocytes.[25–27] It is now becoming increasingly clear that changes in $[Ca^{2+}]_i$ levels not only influence the developmental processes that accompany the transition of OPCs into mature myelinating oligodendrocytes, but also intervene in the initiation of the myelination and re-myelination processes.[21] As regards NCX3 activation during the progression of OPCs into oligodendrocytes, it should be considered that the basal intracellular calcium levels (40–60 nM) we recorded in human M03.13 OPCs deal with the mean values obtained in the whole cytosol. However, it has been reported that, at highly localized intracellular microdomains along the processes of cultured OPCs, intracellular calcium transients may be evoked during the different stages of oligodendrocyte development by several agents, including growth factors (i.e. PDGF, FGF), myelin components, and G-protein-coupled receptor activation.[28,7] These $[Ca^{2+}]_i$, transients reach levels, which are compatible with the kinetics of NCX3 activation.[8] The importance of calcium signaling mediated by NCX3 during oligodendrocyte development and myelin formation is supported by our findings showing that knocking down NCX3 expression and activity by an siRNA strategy in OPC cultures prevented the upregulation of the myelin proteins CNPase and MBP, whereas its overexpression induced the upregulation of these two myelin markers.

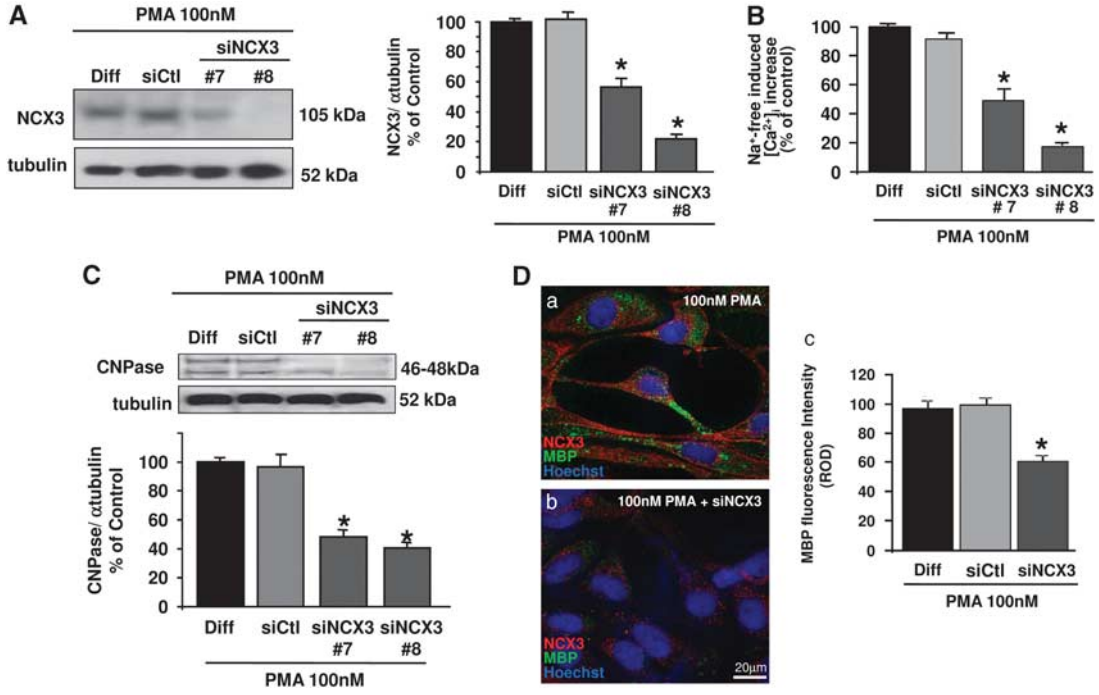

Figure 6 Effect of NCX3 silencing on CNPase and MBP expression. (**A**) Western blot (left) and densitometric analysis (right) of NCX3 protein levels in NCX3-silenced MO3.13 oligodendrocytes with two siRNAs (#7 and #8) after 100 nM PMA exposure for 3 days. (**B**) Quantification of Na^+-free-induced $[Ca^{2+}]_i$ increase measured as Δ% of peak *versus* basal values in NCX3-silenced MO3.13 oligodendrocytes with two siRNAs (#7 and #8) after 100 nM PMA exposure for 3 days. Each bar represents the mean ± S.E.M. of the data obtained from 60 cells per group in three independent experimental sessions. $^*P<0.05$ *versus* differentiated cells (Diff). (**C**) Western blot and densitometric analysis of CNPase protein levels in NCX3-silenced MO3.13 oligodendrocytes with two siRNAs (#7 and #8) after 100 nM PMA exposure for 3 days. The values represent the mean ± S.E.M. ($n=3$–4). $^*P<0.05$ *versus* differentiated cells (Diff). (**D**) Confocal immunofluorescence images showing both NCX3 (red) and MBP immunosignal (green) in differentiated MO3.13 oligodendrocytes incubated in the absence (a) or in the presence (b) of siNCX3. The quantification of MBP fluorescence intensity in differentiated MO3.13 oligodendrocytes incubated in the absence or in the presence of siNCX3 is shown in panel c. The values represent the mean ± S.E.M. ($n=3$–4). $^*P<0.05$ *versus* differentiated cells (Diff). Scale bars: a–b: 20 μm

Currently, as failure of OPC differentiation is significantly associated with impaired myelin sheath regeneration in de-myelinating diseases, the therapeutic opportunity to control OPC progenitor differentiation is believed of critical importance for establishing new repair and regenerative strategies.[4] In the light of our findings, it is possible to speculate that, under different de-myelinating conditions, the activation of the NCX3 exchanger might have a relevant role in the stimulation of the OPC development and re-myelination process. Analysis of myelin proteins and NG2 expression in NCX3-null mice appears to support this hypothesis. Indeed, we found that NCX3-knockout mice show hypo-myelination that is accompanied by an augmented expression of the OPC marker NG2 and a reduction of spinal cord size. NCX3 is most likely not critical for embryonic brain development as the gross cytoarchitecture of neurons,[23] astrocytes, and OPCs was not altered in $ncx3^{-/-}$ mice. More specifically, the hypo-myelinization observed in the NCX3-knockout mice of the present study might be explained by evidence indicating that the formation of myelin is a protracted developmental process extending during the postnatal period.[29] Although further studies during other postnatal ages might provide a more precise time course of the postnatal expressions of myelin markers in $ncx3^{-/-}$ mice, our findings suggest that the decreased myelination in the $ncx3^{-/-}$ mice might be caused by a decrease in the number of differentiated oligodendrocytes and/or by a decreased ability of oligodendrocytes to produce myelin.

Recent evidence also points out that the NCX3 exchanger is a new potential therapeutic target for neuroprotection. Indeed, mice lacking NCX3 by silencing or transgenic approaches, show an enhanced cellular vulnerability to hypoxic-ischemic insults[30] and a worsening of the infarct area after stroke.[12,14] More recently, NCX3 has also been proposed as a new molecular effector involved in the neuroprotective effect of ischemic post-conditioning.[31] In agreement with the beneficial role of this exchanger, it has been demonstrated that NCX3-deficient mice show skeletal muscle fiber necrosis and impaired neuromuscular transmission, which is clinically associated with reduced motor activity, weakness of forelimb muscles, and fatigability.[22] According to our results, the symptoms observed by Sokolow *et al*.[22] in $ncx3^{-/-}$ mice may not only be attributed exclusively to alterations at the neuromuscular junction or the skeletal fibers, but may also result from defects in CNS myelination. The reduced expression of the axonal marker we detected in the spinal cord of $ncx3^{-/-}$ mice seems to further support this hypothesis. In addition, it has been well-documented that hypo-myelination can lead to cognitive impairments.[32] Interestingly, we have recently provided evidence that NCX3-knockout mice show an impairment in hippocampal LTP, spatial learning, and memory.[23]

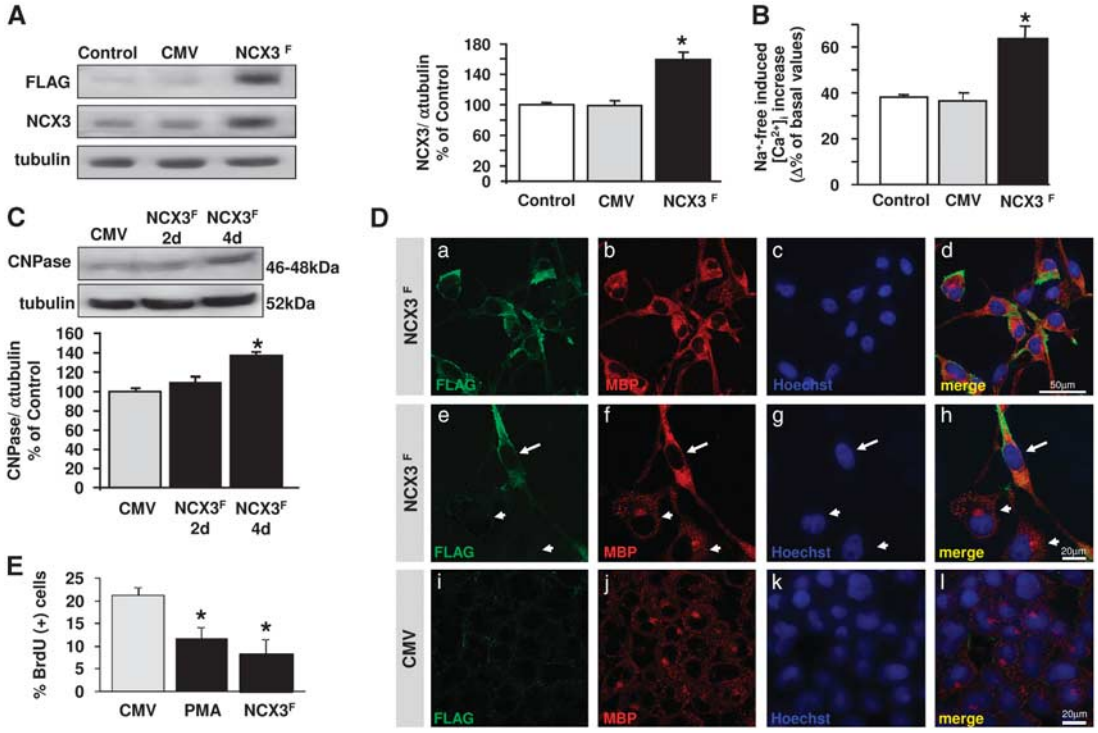

Figure 7 Effect of NCX3 overexpression on CNPase and MBP expression. (**A**, left) Western blot analysis of Flag–NCX3 and NCX3 protein levels detected with anti-Flag and anti-NCX3 antibodies, respectively, in MO3.13 cells 72 h after transfection. (**A**, right) Densitometric analysis of NCX3 protein levels in NCX3-overexpressing MO3.13 oligodendrocytes. The data were normalized on the basis of α-tubulin levels and expressed as percentage of control. The values represent the means ± S.E.M. ($n = 3$–4). *$P < 0.05$ *versus* control. (**B**) Quantification of Na^+-free-induced $[Ca^{2+}]_i$ increase measured as Δ% of peak *versus* basal values in $NCX3^F$-overexpressing MO3.13 oligodendrocytes at 72 h after transfection. Each bar represents the mean ± S.E.M. of the data obtained from 60 cells per group in three independent experimental sessions. *$P < 0.05$ *versus* control. (**C**) Western blot and densitometric analysis of CNPase protein levels in $NCX3^F$-overexpressing MO3.13 oligodendrocytes at 2 and 4 days after transfection. The data were normalized on the basis of α-tubulin levels and expressed as percentage of control. The values represent the means ± S.E.M. ($n = 3$). *$P < 0.05$ *versus* control. (**D**) Colocalization of Flag (green) with MBP (red) in $NCX3^F$-transfected (a–h) and control MO3.13 cells (i–l). Panels e–h show a higher magnification of a single representative Flag-MBP-double-labeled cell (arrow) and two non-transfected cells (arrowheads). Scale bars: a–d: 50 μm; e–l: 20 μm. (**E**) Quantification of the percentage of BrdU-positive cells in control, PMA-exposed, or $NCX3^F$-transfected cells. The data are expressed as percentages of total Hoechst-positive nuclei. *$P < 0.05$ *versus* control cells

Overall, our findings, by providing new insights into the molecular and cellular mechanisms involved in OPC development, demonstrate for the first time that calcium signaling mediated by the NCX3 isoform is crucially involved in oligodendrocyte maturation and myelin formation. Further studies are nonetheless required to reveal whether alterations in NCX3 activity might contribute to OPC dysfunction in de-myelinating diseases, and whether its modulation might be therapeutically relevant.

Materials and Methods

Animals: Wild-type $ncx3^{+/+}$ and knockout $ncx3^{-/-}$ mice[22] (provided by Dr. S Sokolow (UCLA School of Nursing, Los Angeles, CA, USA) and Dr. A Herchuelz (Faculté de Médecine, Université Libre de Bruxelles, Brussels, Belgium)) aged 3–4 months were housed in a temperature- and humidity-controlled colony room under diurnal lighting conditions. Animal handling was in accordance with the International Guidelines for Animal Research and the experimental protocol was approved by the Animal Care and Use Committee of 'Federico II' University of Naples.

Cell cultures

The human oligodendrocyte MO3.13 cell line and in vitro differentiation: The MO3.13 cell line is an immortalized human clonal model that expresses the phenotypic characteristics of OPCs.[33] Cells were cultured in Dulbecco's modified Eagle's medium (DMEM) supplemented with 10% fetal bovine serum (FBS), 100 U/ml penicillin, 10 μg/ml streptomycin, and 2 mmol/l L-glutamine (MO3.13 medium). To induce an oligodendrocyte phenotype, human MO3.13 cells were cultured in a serum-free chemically defined medium composed of DMEM supplemented with 500 μg/l insulin, 100 μg/ml human transferrin, 0.52 μg/l sodium selenite, 0.63 μg/ml progesterone, 16.2 μg/ml putrescin, 100 U/ml penicillin, 100 μg/ml streptomycin, 2 mM glutamine (OPC medium), and containing 100 nM PMA for 7 days *in vitro* (DIVs). Fresh PMA was added every time the culture medium was changed. To induce astrocyte phenotypes, human MO3.13 cells were cultured in MO3.13 medium for 7 DIVs.

Primary rat OPC cultures and in vitro differentiation: Purified OPC cultures were prepared as described by McCarthy and de Vellis.[34] In brief, primary rat mixed glial cell cultures were isolated from the cerebral cortex of postnatal day 1 rats, dissociated into single cells, and cultured into poly-D-lysine (Sigma-Aldrich, St. Louis, MO, USA)-coated tissue culture flasks in MO3.13 medium at 37 °C in a humidified, 5% CO_2 incubator.[9] Once confluent (after 7–9 days), the microglia were separated by mechanical shaking of flasks on a rotary shaker for 60 min at 200 r.p.m. and removed. The cultures were then subjected to an additional 16 h of shaking at 200 r.p.m. To minimize contamination by microglial cells, the suspension of detached cells was incubated twice for 40 min at room temperature (RT). The non-adhering OPCs were plated into poly-D-lysine-coated plates in MO3.13 medium and maintained at 37 °C in a humidified, CO_2 atmosphere. This procedure yields 98% A2B5-positive cells. Five hours after plating, the culture medium was replaced with OPC medium supplemented with 10 ng/ml PDGF-AA and 10 ng/ml bFGF to maintain the undifferentiated state and support OPC survival. Then, to facilitate the differentiation of precursors into oligodendrocytes, PDGF and bFGF were withdrawn from the OPC medium, which were instead supplemented with either

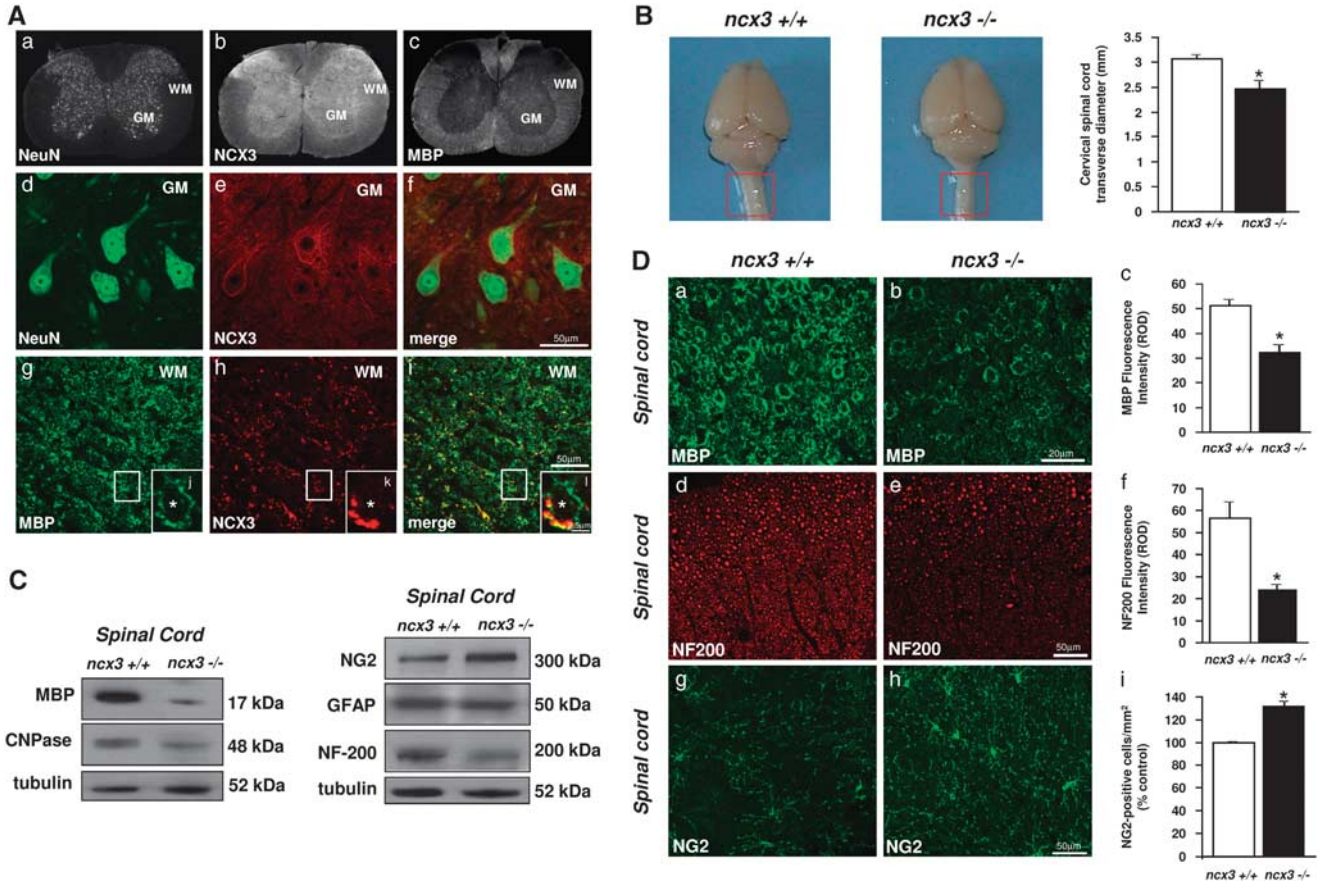

Figure 8 Expression of OPC, oligodendrocyte, astrocyte, and axonal markers in the spinal cord of ncx3$^{+/+}$ and ncx3$^{-/-}$ mice. (**A**) Distribution of NeuN (a), NCX3 (b), and MBP (c) immunoreactivities in the spinal cord of ncx3$^{+/+}$ mice. Colocalization of NCX3 with NeuN in the gray matter (d–f), or with MBP in the white matter (g–i), of ncx3$^{+/+}$ spinal cord sections. (j–l) High-magnification images of the frame depicted in panels (g–i) illustrating co-expression of MBP with NCX3 immunosignals around a single axon (asterisk). Scale bars in A: d–i: 50 μm; j–l: 2,5 μm. (**B**) Representative images of 4-month ncx3$^{+/+}$ (left) and ncx3$^{-/-}$ (middle) whole-brain and spinal cord samples. The red boxes indicate the reduction in spinal cord size between ncx3$^{+/+}$ and ncx3$^{-/-}$ mice. Transverse measurements of the cervical spinal cord diameter in ncx3$^{+/+}$ and ncx3$^{-/-}$ (left). The values represent the means ± S.E.M. ($n = 6$). *$P < 0.05$ *versus* ncx3$^{-/-}$. (**C**) Western blotting of MBP, CNPase, NG2, GFAP, and NF200 in ncx3$^{+/+}$ and ncx3$^{-/-}$ mice. (**D**, a–c) Distribution of MBP immunoreactivity (a–b) and quantification of its fluorescence intensity (c) in the white matter of the spinal cord from ncx3$^{+/+}$ and ncx3$^{-/-}$ mice. (**D**, d–f) Distribution of NF-200 immunoreactivity (d–e) and quantification of its fluorescence intensity (f) in the white matter of the spinal cord from ncx3$^{+/+}$ and ncx3$^{-/-}$ mice. (**D**, g–i) Distribution of NG2 immunoreactivity (g–h) and quantification of NG2-positive cells (i) in the white matter of the spinal cord from ncx3$^{+/+}$ and ncx3$^{-/-}$ mice. For cell counting, 6–10 microscope fields were counted for each section and six sections for each animal were analyzed. NG2 cell quantification has been calculated in the total area as the number of cells per mm^2 and reported as percentage of NG2-positive cells in ncx3$^{-/-}$ *versus* ncx3$^{+/+}$ (control). The values represent the means ± S.E.M. ($n = 3$–4). *$P < 0.05$ *versus* ncx3$^{+/+}$. Scale bars in D: a, b: 20 μm; d, e, 50 μm; g, h: 50 μm

30 ng/ml T3 and 40 ng/ml T4 for 7 days. For electrophysiological and microfluorimetric experiments, cells were seeded on glass coverslips coated with 30 ng/ml poly-D-lysine.

Quantitative real-time RT-PCR: Total RNA was extracted from human MO3.13 cells using Trizol (Invitrogen, Milan, Italy). After DNase-I treatment (1 U/μl; Sigma-Aldrich) for 15 min at RT, the first-strand cDNA was synthesized using 5 μg of the total RNA and 500 ng of random primers by using the SuperScript (high-capacity cDNA RT kit; Applied Biosystems, Monza, Italy). Using 1/10 of the cDNAs as a template, quantitative real-time PCR was performed in a 7500 fast real-time PCR system (Applied Biosystems) by using the Fast SYBR Green Master Mix (cod. 4385610; Applied Biosystems). Samples were amplified simultaneously in triplicate in one assay run for 40 cycles with a single fluorescence measurement. PCR data were then collected by using the ABI Prism 7000 SDS software (Applied Biosystems). Afterwards, the products were electrophoretically separated on 3% agarose gels and bands were visualized with ethidium bromide and documented by using the Gel Doc Imaging System (Bio-Rad, Hercules, CA, USA). Normalization of data was performed by using ribosomal protein L19 as an internal control; differences in mRNA content between groups were calculated as normalized values by using the $2_t^{-\Delta\Delta C}$ formula and the results were tested for significance by using the Relative Expression Software Tool (REST).[35] The oligonucleotide sequences were as follows: NCX1: 5′-CTGGAGCGCGAGGAAATGTTA-3′ and 5′-GACGGGGTTCT CCAATCT-3′; NCX2: 5′-AGGAGGCCGCACACCTTTCC-3′ and 5′-CAAGGCGTG GCTGGGCTCTC-3′; NCX3: 5′-GGCTGCACCATTGGTCTCA-3′ and 5′-GACGGG GTTCTCCAATCT-3′; and L19: 5′-CTAGTGTCCTCCGCTGTGG-3′ and 5′-AAGGT GTTTTTCCGGCATC-3′.

Western blotting: Protein samples were separated on 8 or 14% polyacrylamide gel and electrophoretically transferred onto nitrocellulose membranes. Filters were probed using the indicated primary antibodies: monoclonal anti-NCX1 (1 : 500; Swant, Bellinzona, Switzerland), polyclonal anti-NCX3 (1 : 4000; provided by Dr. KD Philipson and Dr. DA Nicoll, Los Angeles, CA, USA), polyclonal anti-CNPase (1 : 400; Santa Cruz Biotechnology Inc., Santa Cruz, CA, USA); monoclonal anti-MAG (1 : 1000; Millipore, Milan, Italy); polyclonal anti-MBP (1 : 200; Millipore) monoclonal anti-MBP (1 : 200; Covance, Princeton, NJ, USA); and monoclonal anti-Flag (1 : 2000; Sigma, Milan, Italy), polyclonal anti-NG2 (1 : 1000; Millipore), polyclonal anti-GFAP (1 : 1000; Sigma), polyclonal anti-NF-200 (1 : 1000; Sigma), monoclonal anti-α-tubulin (1 : 1000; Sigma). Proteins were visualized with peroxidase-conjugated secondary antibodies, using the enhanced chemiluminescence system (Amersham-Pharmacia Biosciences LTD, Uppsala, Sweden).

Confocal immunofluorescence analysis: Confocal immunofluorescence procedures in cells or sections were performed as described previously.[9,36,37] Mice were anesthetized intraperitoneally with chloral hydrate (300 mg/kg) and perfused transcardially with 4% wt/vol. paraformaldehyde and 15% wt/vol. picric acid in phosphate buffer. Cervical spinal cords were cryoprotected in sucrose, frozen in OCT, and sectioned coronally at 40 μm on a cryostate. Cell cultures were fixed in 4% wt/vol. paraformaldehyde in phosphate buffer for 30 min. After blocking, sections or cells were incubated with primary antibodies for 24 or 48 h, respectively. The primary antibodies used in these experiments were the following: monoclonal anti-NCX1 (1 : 500; Swant), polyclonal anti-NCX3 (1 : 4000; provided by Dr. Philipson), monoclonal anti-MAG (1 : 500; Millipore), polyclonal anti-CNPase (1 : 200; Santa Cruz Biotechnology Inc.), polyclonal anti-MBP (1 : 2000; Millipore), monoclonal anti-MBP (1 : 400; Covance), monoclonal anti-S100B (1 : 1000; Sigma), polyclonal anti-GFAP (1 : 1000; Sigma), polyclonal anti-NG2 (1 : 1000; Millipore), monoclonal anti-Golgin-97 (1 : 200; Molecular Probes, Eugene, OR, USA), monoclonal anti-Flag (1 : 2000; Sigma), polyclonal anti-NF200 (1 : 1000; Sigma), polyclonal anti-PDGFαR (1 : 200; Santa Cruz Biotechnology Inc.). OPC progenitors were also identified by using the A2B5 conjugated to fluorescein isothiocyanate (1 : 4000; Millipore). Subsequently, sections or cells were incubated with corresponding fluorescence-labeled secondary antibodies (Alexa-488- or Alexa-594-conjugated anti-mouse or anti-rabbit IgGs). Images were observed using a Zeiss LSM510 META/laser-scanning confocal microscope. Single images were taken with an optical thickness of 0.7 μm and a resolution of 1024 $\times$ 1024.

The MBP and NF-200 fluorescence intensity on coronal tissue sections from spinal cord in ncx3$^{+/+}$ and ncx3$^{-/-}$ mice was quantified in terms of pixel intensity value by using the NIH image software, as described previously.[13,23] All images were obtained with a $\times$ 20 objective or $\times$ 40 with identical laser power settings. The number of NG2 cells was determined in the white matter of spinal cord of ncx3$^{+/+}$ and ncx3$^{-/-}$ mice by manual counting at $\times$ 40 magnification. Only NG2 cells with clearly a visible cell body and profiles were counted. Four mice per group were included in the studies, and six slices from every mouse were analyzed.

BrdU immunohistochemistry: Proliferation was assessed by using BrdU labeling (Sigma-Aldrich). After 48 h of transfection, cells were double-pulsed with BrdU (every 6–8 h) for an additional 24 h at a final concentration of 10 μM at 37 °C. After fixation in 4% PAF for 30 min, cellular DNA was denatured with 2 N HCl for 30 min at 37 °C. Cells were first washed in 0.1 M borate buffer (pH 8.5) and then, after blocking in 3% BSA for 40 min, incubated overnight with a polyclonal sheep anti-BrdU antibody (1 : 1000; Abcam, Cambrige, UK) at 4 °C. After rinsing with PBS, the cultures were incubated with the corresponding biotinylated secondary antibody (1 : 200; Vector Labs, Burlingame, CA, USA) for 1 h and in Elite ABC (1 : 300 dilution; Vector Labs) for 90 min. The peroxidase reaction was developed by using 3,3-diaminobenzidine-4HCl as a chromogen. After the final wash, sections were coverslipped and processed for microscope analysis. Total cell nuclei were stained with Hoechst-33258 (Sigma). To quantify the number of BrdU-positive cells, bright-field images of BrdU-positive cells were captured at $\times$ 40 magnification. Then cells were counted in six non-overlapping microscope fields from three coverslips of each cell group. The data were expressed as percentages of total Hoechst-positive nuclei.

Electrophysiology: I_{NCX} was recorded from MO3.13. cells and primary OPC cultures by the patch-clamp technique in whole-cell configuration as described previously.[9] The Ringer solution contained 20 mmol/l tetraethylammonium, 1 mmol/l 4-aminopiridine, 50 nmol/l tetrodotoxin, 10 μmol/l nimodipine, and 50 μmol/l Ba^{2+} to block tetraethylammonium- and 4-aminopiridine-sensitive K^+, tetrodotoxin-sensitive Na^+, L-type Ca^{2+}, and K_{ir} currents.

$[Ca^{2+}]_i$ measurement: $[Ca^{2+}]_i$ was measured by single-cell FURA-2 acetoxymethyl-ester video-imaging, as described previously.[30] Cells were loaded with 6 μmol/l FURA-2 acetoxymethyl-ester for 30 min at 37 °C in normal Krebs solution. Then, coverslips were placed into a perfusion chamber (Medical System Co., Greenvale, NY, USA) mounted onto the stage of an inverted Zeiss Axiovert 200 microscope (Carl Zeiss, Milan, Italy) equipped with a FLUAR $\times$ 40 oil objective lens. After loading, cells were alternatively illuminated at wavelengths of 340 and 380 nm by a Xenon lamp. NCX activity was evaluated as Ca^{2+} uptake through the reverse mode by switching the normal Krebs medium to an Na^+-deficient NMDG + medium (Na^+-free).

NCX3 silencing and overexpression: Silencing of NCX3 in MO3.13 cells was performed by using the HiPerFect Transfection kit (Qiagen, Milan, Italy), by using two different FlexiTube siRNAs for NCX3, (#7) Hs_SLC8A3_7 (5′-ACC ATTGGtCTCAAAGATTCA-3′) and (#8) Hs_Slc8A3_8 (5′-CACCACGCTC TTGCTTCCTAA-3′), and a validated irrelevant AllStars siRNA as a negative control (siCtl). Cells were incubated with OptiMEM (Invitrogen) supplemented with the RNAiFect Transfection Reagent (Qiagen) and 20 nM of each siRNA duplex for 15 h. Then, cells were incubated in culture medium for an additional 48–96 h. The construct expressing NCX3–Flag (GeneCopeia, Rockville, MD, USA) was transiently transfected with a standard procedure using Lipofectamine 2000 (Invitrogen).[9]

Statistical analysis: The data are expressed as the mean $\pm$ S.E.M. of the values obtained in three separate experiments. Statistical comparisons between controls and treated groups were performed by one-way analysis of variance followed by Newman–Keuls' test. $P < 0.05$ was considered significant.

Conflict of Interest

The authors declare no conflict of interest.

Acknowledgements. This work was supported by the following grants: COFIN 2008; Ricerca Sanitaria RF-FSL352059 Ricerca finalizzata 2006; Ricerca Oncologica 2006; Progetto Strategico 2007; Progetto Ordinario 2007 (all to L Annunziato). We thank Dr S Sokolow (UCLA School of Nursing, Los Angeles, CA, USA) and Dr A Herchuelz (Université Libre de Bruxelles, Faculté deMédecine, Brussels, Belgium) for providing the ncx3$^{-/-}$ mice. We also thank Dr. Paola Merolla for the editorial revision, and Dr Claudia Savoia, Mr Vincenzo Grillo, and Mr Carmine Capitale for technical support.

1. Chong SY, Chan JR. Tapping into the glial reservoir: cells committed to remaining uncommitted. *J Cell Biol* 2010; **188**: 305–312.
2. Nishiyama A, Komitova M, Suzuki R, Zhu X. Polydendrocytes (NG2 cells): multifunctional cells with lineage plasticity. *Nat Rev Neurosci* 2009; **10**: 9–22.
3. Rivers LE, Young KM, Rizzi M, Jamen F, Psachoulia K, Wade A *et al.* PDGFRA/NG2 glia generate myelinating oligodendrocytes and piriform projection neurons in adult mice. *Nat Neurosci* 2008; **11**: 1392–1401.
4. Franklin RJ, French-Constant C. Remyelination in the CNS: from biology to therapy. *Nat Rev Neurosci* 2008; **9**: 839–855.
5. Barres BA, Koroshetz WJ, Swartz KJ, Chun LL, Corey DP. Ion channel expression by white matter glia: the O-2A glial progenitor cell. *Neuron* 1990; **4**: 507–524.
6. Kettenmann H, Kirischuk S, Verkhratsky A. Calcium signalling in oligodendrocytes. *Neurophysiology* 1994; **26**: 26–31.
7. Soliven B. Calcium signalling in cells of oligodendroglial lineage. *Microsc Res Tech* 2001; **52**: 672–679.
8. Annunziato L, Pignataro G, Di Renzo GF. Pharmacology of brain Na^+/Ca^{2+} exchanger: from molecular biology to therapeutic perspectives. *Pharmacol Rev* 2004; **56**: 633–654.
9. Boscia F, Gala R, Pannaccione A, Secondo A, Scorziello A, Di Renzo G *et al.* NCX1 expression and functional activity increase in microglia invading the infarct core. *Stroke* 2009; **40**: 3608–3617.
10. Craner MJ, Hains BC, Lo AC, Black JA, Waxman SG. Co-localization of sodium channel Nav1.6 and the sodium–calcium exchanger at sites of axonal injury in the spinal cord in EAE. *Brain* 2004; **127** (Part 2): 294–303.
11. Craner MJ, Newcombe J, Black JA, Hartle C, Cuzner ML, Waxman SG. Molecular changes in neurons in multiple sclerosis: altered axonal expression of Nav1.2 and Nav1.6 sodium channels and Na+/Ca2+ exchanger. *Proc Natl Acad Sci USA* 2004; **101**: 8168–8173.
12. Pignataro G, Gala R, Cuomo O, Tortiglione A, Giaccio L, Castaldo P *et al.* Two sodium/calcium exchanger gene products, NCX1 and NCX3, play a major role in the development of permanent focal cerebral ischemia. *Stroke* 2004; **35**: 2566–2570.
13. Boscia F, Gala R, Pignataro G, de Bartolomeis A, Cicale M, Ambesi Impiombato A *et al.* Permanent focal brain ischemia induces isoform-dependent changes in the pattern of Na^+/Ca^{2+} exchanger gene expression in the ischemic core, periinfarct area, and intact brain regions. *J Cereb Blood Flow Metab* 2006; **26**: 502–517.
14. Molinaro P, Cuomo O, Pignataro G, Boscia F, Sirabella R, Gala R *et al.* Targeted disruption of NCX3 gene leads to a worsening of ischemic brain damage. *J Neurosci* 2008; **28**: 1179–1184.
15. Li S, Jiang Q, Stys PK. Important role of reverse Na(+)–Ca(2+) exchange in spinal cord white matter injury at physiological temperature. *J Neurophysiol* 2000; **84**: 1116–1119.
16. Tomes DJ, Agrawal SK. Role of Na(+)–Ca(2+) exchanger after traumatic or hypoxic/ischemic injury to spinal cord white matter. *Spine J* 2002; **2**: 35–40.
17. Nicoll DA, Sondoni S, Philipson KD. Molecular cloning and functional expression of the cardiac sarcolemmal Na^+–Ca^{2+} exchanger. *Science* 1990; **250**: 562–565.

18. Li Z, Matsuoka S, Hryshko LV, Nicoll DA, Bersohn MM, Burke EP. Cloning of the NCX2 isoform of the plasma membrane Na^+–Ca^{2+} exchanger. *J Biol Chem* 1994; **269**: 17434–17439.
19. Nicoll DA, Quednau BD, Qui Z, Xia YR, Lusis AJ, Philipson KD. Cloning of a third mammalian Na^+–Ca^{2+} exchanger, NCX3. *J Biol Chem* 1996; **271**: 24914–24921.
20. Quednau BD, Nicoll DA, Philipson KD. Tissue specificity and alternative splicing of the Na^+/Ca^{2+} exchanger isoforms NCX1, NCX2, and NCX3 in rat. *Am J Physiol* 1997; **272** (4 Part 1): C1250–C1261.
21. Paez PM, Fulton D, Colwell CS, Campagnoni AT. Voltage-operated Ca(2+) and Na(+) channels in the oligodendrocyte lineage. *J Neurosci Res* 2009; **87**: 3259–3266.
22. Sokolow S, Manto M, Gailly P, Molgó J, Vandebrouck C, Vanderwinden JM *et al.* Impaired neuromuscular transmission and skeletal muscle fiber necrosis in mice lacking Na/Ca exchanger 3. *J Clin Invest* 2004; **113**: 265–273.
23. Molinaro P, Viggiano D, Nisticò R, Secondo A, Boscia F, Pannaccione A *et al.* NCX3 (Na^+–Ca^{2+} exchanger) knock-out mice display an impairment in hippocampal long-term potentiation and spatial learning and memory. *J Neurosci* 2011; **31**: 7312–7321.
24. Tong XP, Li XY, Zhou B, Shen W, Zhang ZJ, Xu TL *et al.* Ca(2+) signaling evoked by activation of Na(+) channels and Na(+)/Ca(2+) exchangers is required for GABA-induced NG2 cell migration. *J Cell Biol* 2009; **186**: 113–128.
25. Raizman JE, Komljenovic J, Chang R, Deng C, Bedosky KM, Rattan SG *et al.* The participation of the Na+–Ca2+ exchanger in primary cardiac myofibroblast migration, contraction, and proliferation. *J Cell Physiol* 2007; **213**: 540–551.
26. Touyz RM, Schiffrin EL. Growth factors mediate intracellular signaling in vascular smooth muscle cells through protein kinase C-linked pathways. *Hypertension* 1997; **30**: 1440–1447.
27. Iwamoto T, Wakabayashi S, Shigekawa M. Growth factor-induced phosphorylation and activation of aortic smooth muscle Na^+/Ca^{2+} exchanger. *J Biol Chem* 1995; **270**: 8996–9001.
28. Butt AM. Neurotransmitter-mediated calcium signalling in oligodendrocyte physiology and pathology. *Glia* 2006; **54**: 666–675.
29. Baumann N, Pham-Dinh D. Biology of oligodendrocyte and myelin in the mammalian central nervous system. *Physiol Rev* 2001; **81**: 871–927.
30. Secondo A, Staiano IR, Scorziello A, Sirabella R, Boscia F, Adornetto A *et al.* The Na^+/Ca^{2+} exchanger isoform 3 (NCX3) but not isoform 2 (NCX2) and 1 (NCX1) singly transfected in BHK cells plays a protective role in a model of *in vitro* hypoxia. *Ann NY Acad Sci* 2007; **1099**: 481–485.
31. Pignataro G, Esposito E, Cuomo O, Sirabella R, Boscia F, Guida N *et al.* The NCX3 isoform of the Na^+/Ca^{2+} exchanger contributes to neuroprotection elicited by ischemic postconditioning. *J Cereb Blood Flow Metab* 2011; **31**: 362–370.
32. Nave KA. Myelination and support of axonal integrity by glia. *Nature* 2010; **468**: 244–252.
33. McLaurin J, Trudel GC, Shaw IT, Antel JP, Cashman NR. A human glial hybrid cell line differentially expressing genes subserving oligodendrocyte and astrocyte phenotype. *J Neurobiol* 1995; **26**: 283–293.
34. McCarthy KD, de Vellis J. Preparation of separate astroglial and oligodendroglial cell cultures from rat cerebral tissue. *J Cell Biol* 1980; **85**: 890–902.
35. Pfaffl MW. A new mathematical model for relative quantification in real-time RT-PCR. *Nucleic Acids Res* 2001; **29**: e45.
36. Boscia F, Ferraguti F, Moroni F, Annunziato L, Pellegrini-Giampietro DE. mGlu1alpha receptors are co-expressed with CB1 receptors in a subset of interneurons in the CA1 region of organotypic hippocampal slice cultures and adult rat brain. *Neuropharmacology* 2008; **55**: 428–439.
37. Boscia F, Esposito CL, Di Crisci A, de Franciscis V, Annunziato L, Cerchia L. GDNF selectively induces microglial activation and neuronal survival in CA1/CA3 hippocampal regions exposed to NMDA insult through Ret/ERK signalling. *PLoS One* 2009; **4**: e6486.

Supplementary Information accompanies the paper on Cell Death and Differentiation website (http://www.nature.com/cdd)